Chemical Geology 702 (2026) 123218

Contents lists available at ScienceDirect

Chemical Geology

journal homepage: www.elsevier.com/locate/chemgeo

Mercury concentration: A new window into ancient diets and trophic levels in vertebrate paleontology

Felipe M.S. Cardia [a,b], José Vicente E. Bernardi [c], Carlos Eduardo M. Oliveira [d,o], Marco B. Andrade [e], Max C. Langer [f], Sandra A.S. Tavares [g], Fabiano V. Iori [h], William R. Nava [i], Thiago S. Marinho [j,k,l], Luiz Carlos B. Ribeiro [j,k,l], Jurandir R. Souza [a], Rodrigo M. Santucci [c,m,n,*]

[a] Instituto de Química, Universidade de Brasília, Distrito Federal, Brazil
[b] Faculdade de Medicina, Universidade de Brasília, Distrito Federal, Brazil
[c] Faculdade UnB Planaltina, Universidade de Brasília, Distrito Federal, Brazil
[d] Instituto Federal de Educação, Ciência e Tecnologia de São Paulo, Campus Votuporanga (IFSP), São Paulo, Brazil
[e] Pontifícia Universidade Católica do Rio Grande do Sul, Porto Alegre, Brazil
[f] Departamento de Biologia, FFCLRP, Universidade de São Paulo, Ribeirão Preto, Brazil
[g] Museu de Paleontologia Prof. Antonio Celso de Arruda Campos, Monte Alto, São Paulo, Brazil
[h] Museu de Paleontologia Pedro Candolo, Uchoa, São Paulo, Brazil
[i] Museu de Paleontologia de Marília, Marília, São Paulo, Brazil
[j] Centro de Pesquisas Paleontológicas L. I. Price, Complexo Cultural e Científico Peirópolis, Universidade Federal do Triângulo Mineiro, Minas Gerais, Brazil
[k] Instituto de Ciências Exatas, Naturais e Educação, Universidade Federal do Triângulo Mineiro, Minas Gerais, Brazil
[l] Uberaba Unesco Global Geopark, Brazil
[m] Instituto de Ciências Biológicas, Universidade de Brasília, Distrito Federal, Brazil
[n] Instituto de Geociências, Universidade de Brasília, Distrito Federal, Brazil
[o] Museu de Paleontologia de Fernandópolis Prof. Cristovão Souza de Oliveira, Fernandópolis, São Paulo, Brazil

ARTICLE INFO

Editor: Dr. Vasileios Mavromatis

Keywords:
Biomagnification
Mercury (Hg)
Fossil vertebrates
Bauru Group
Trophic level

ABSTRACT

Direct evidence about feeding habits and trophic levels of extinct species is scarce in the fossil record. Typically, such information is based on geochemistry, stomach contents, anatomy, and, whenever possible, comparison with living counterparts. Despite the challenges involved, such reconstructions are vital for understanding the structure of past ecosystems. Here, we propose a novel geochemical approach in paleontology that uses total mercury concentration (THg) in fossil vertebrate tissues (bones and tooth enamel) and its bioaccumulation and biomagnification properties as geochemical indicators for the inference of feeding habits and trophic levels. Thin section and X-ray diffractometry (XRD) revealed that THg values found in bioapatite from the diverse and well-preserved fossil vertebrates of the Upper Cretaceous Bauru Group (Brazil) are not altered by diagenetic processes. The results show that each vertebrate group analyzed (e.g., fishes, turtles, amphibians, crocodylomorphs, avian, and non-avian dinosaurs) are characterized by different THg concentrations (ranging from 1.66 to 15 ng.g^{-1} Hg). Notably, similar values were found in fossils of the same taxonomic group regardless of their geological unit of origin. More importantly, taxa with different feeding habits were positioned at different trophic levels based on the bioaccumulation and biomagnification of Hg. Reliable Hg analyses in fossils require confirming that bones are free from diagenetic contamination that may artificially elevate their Hg concentrations.

1. Introduction

Except for exceptionally rare findings of stomach content (e.g. Brown et al., 2020; Godoy et al., 2014; Maisey, 1994; Mulder, 2013; O'Connor et al., 2011; O'Keefe et al., 2009; Xing et al., 2012), the feeding habits and trophic position of fossil vertebrates can be only indirectly inferred from their morphology, comparisons with extant related forms (Meloro et al., 2015), geochemical analyses of tooth and bone bioapatite, like carbon (e.g. Ambrose and Krigbaum, 2003; Fricke, 2007; Koch, 2007; Kolodny et al., 1996; Thorp and Van Der Merwe, 1987; Wang and Cerling, 1994) and, more recently, enamel-bound nitrogen (e.g. Comans et al., 2024; Kast et al., 2022; Lüdecke et al., 2025; Moubtahij et al.,

* Corresponding author at: Faculdade UnB Planaltina, Universidade de Brasília, Distrito Federal, Brazil.
E-mail address: rodrigoms@unb.br (R.M. Santucci).

https://doi.org/10.1016/j.chemgeo.2025.123218
Received 30 August 2025; Received in revised form 17 December 2025; Accepted 19 December 2025
Available online 22 December 2025

2024), calcium and strontium (e.g. Heuser et al., 2011; Martin et al., 2015, 2017; Michailow et al., 2025; Weber et al., 2025), and zinc (e.g. Bourgon et al., 2021; McCormack et al., 2022, 2025) stable isotopes.

A growing number of new isotopic techniques have been recently proposed to analyze the trophic position of fossil vertebrates (see examples cited above). Yet, except for more recent fossil material that did not endure significant diagenetic alteration, such studies can only be safely performed on tooth enamel or some kinds of fish scales. This is because they are the vertebrate biomineralized tissues with the lowest porosity and least susceptibility to diagenetic alteration (Ambrose and Krigbaum, 2003; Fricke, 2007; Koch, 2007; Thorp and Van Der Merwe, 1987). Thus, putative diagenetic alteration constrains the application of stable-isotope analyses in toothless vertebrates, such as in some fish, turtles, ichthyosaurs, and birds. Therefore, a technique for trophic position inference applicable not only to dental enamel, but also to bone becomes an important complement to isotopic studies in fossils.

In modern ecosystems, due to its global biogeochemical cycle, mercury (Hg) bioaccumulates and biomagnifies in living organisms along the trophic chain (Atwell et al., 1998; Lavoie et al., 2013; Mason et al., 1995; Morel et al., 1998; Selin, 2009). Therefore, the trophic hierarchy of species sharing the same habitat can be estimated based on the quantification of Hg (Atwell et al., 1998). Indeed, studies in Namibian rivers, have shown that crocodiles, despite having one third of the body mass of hippopotamuses (which are herbivores), exhibit three times more Hg in their liver and kidneys (Almli et al., 2005). In King George Island (Antarctica), quantitative information recovered from soil, coastal sediments, and organisms revealed Hg biomagnification along the trophic chain, with low values for plants, invertebrates, and fish, and relatively high Hg concentrations in bird feathers and mammalian fur (Santos et al., 2006).

Although it is not possible to establish a direct relation between present-day and past atmospheric Hg levels, Hg concentrations in marine sediments can be used as a proxy, providing a minimal comparative baseline. In this context, even though modern marine sediments exhibit a slight increase in Hg concentration in the last decades (e.g., Aksentov et al., 2021) and aside minor temporal fluctuations along the Phanerozoic, overall Hg values have remained within an approximate range of 20–150 ppb (Font et al., 2016; Jones et al., 2017; Percival et al., 2017; Shen et al., 2020; Thibodeau et al., 2016).

The presence of Hg in sedimentary rocks has been partially related to the formation of Large Igneous Provinces (LIPs), which affected fossil biotas and may be linked to mass extinctions (Bergquist, 2017; Font et al., 2016; Jones et al., 2017; Liu et al., 2025; Percival et al., 2017; Thibodeau et al., 2016). Hence, Hg has been likely present in the environment for millions of years, bioaccumulating and biomagnifying through trophic webs along the Earth history, impacting distinct paleoecosystems.

Studies show that Hg can replace Ca in different biomineralized tissues like bones and teeth (bioapatite) and biogenetic carbonate of mollusk shell (Ávila et al., 2014; Brown et al., 2005; Jeffree et al., 1995; Meyer et al., 2019; Yap et al., 2003, see also the Discussion section for a more detailed explanation). This is reinforced by recent findings of Hg in the bioapatite of crocodyliform bones from the Cretaceous of Brazil (Cardia et al., 2018), showing higher total mercury concentration (THg) values in fossil material compared to those of the host rocks, indicating that the element was not incorporated to fossil bone due to diagenetic alteration.

Here, we use this rationale to evaluate total mercury concentration in fossil vertebrate bones and teeth as a chemical marker to infer their feeding habits and trophic level position. As a model, we employ the well-known Upper Cretaceous fauna of the Bauru Group, in southeastern Brazil. The Bauru Group (Fernandes and Coimbra, 2000; Batezelli, 2017; Tcacenco-Manzano and Fernandes, 2024) has ideal candidates for this kind of study given its diverse vertebrate fossil record, which includes well-preserved fishes, amphibians, testudines, crocodyliforms, dinosaurs (sauropods and theropods), birds, and mammals (Godoy et al., 2014; Bertini et al., 1993; Carvalho et al., 2004; Castro et al., 2018; Chiappe et al., 2022; Delcourt et al., 2024; França and Langer, 2005; Langer et al., 2022; Martins et al., 2024; Nava and Martinelli, 2011; Pinheiro et al., 2023; Santos et al., 2023; Ruiz et al., 2021; Santucci and Filippi, 2022).

2. Material and methods

2.1. Sampled material

The analyzed materials comprise various vertebrate taxa: Lepisosteidae (1), Anura (1), Pleurodira (3), Crocodylomorpha (Peirosauridae (5), Sphagesauria (11), and Baurusuchidae (8)), Dinosauria (Titanosauria (12), Abelisauridae (3), and Aves (1)) from different units of the Bauru Group (Adamantina, Uberaba, Marília, and Serra da Galga formations). A total of 45 tissue samples were analyzed, including ganoid scales, bones (cortex), and teeth (enamel). For bone samples, only the cortical region was collected, avoiding the more internal, porous areas, of spongy tissue, which are more prone to contain diagenetic minerals.

Additionally, Avery et al. (2023) reported variations in Hg concentration between different bone tissues (cortical and spongy) in archaeological remains of fur seals and sea lions. To minimize potential bias, the same type of bone tissue was consistently sampled. In addition, 15 rock samples associated with some of the analyzed fossils were also examined. For complete information on the sampled materials, including tissue type, taxonomic affinity, locality, geological unit, ontogenetic stage of the individual, and repository institutions see Supplementary Information 1.

As the samples analyzed in this study were stored in different collections for varying periods of time, the superficial layer of both bone and rock specimens was removed prior to the analysis to minimize any potential bias from modern atmospheric Hg contamination.

2.2. Thin sectioning and X-ray diffraction

To evaluate the integrity of the material analyzed in this study, samples of scales, bones, and teeth of different taxa and Bauru Group units were analyzed under X-ray diffraction (Fig. 1). All samples were grounded to a fine powder and analyzed in an X-ray diffractometer (RIGAKU Ultima IV), using 35 kV and 15 mA, at the Institute of Geosciences of the University of Brasília. The scanning protocol was set to 5/min (velocity), 0.05 stepping with 2Θ varying between 2 and 80°. Diffractogram analyses considered the position, width, and sharpness of the peak in different samples of the mineralized tissues.

Furthermore, we thin sectioned different fossil tissues (crocodylomorph bones and eggshells) and rocks (Adamantina, Marília, and Serra da Galga formations) from various Bauru Group sites (Fig. 2). They were observed under polarized light in standard thin sections, where grain margins, birefringence, and signs of dissolution and recrystallization were evaluated. Additionally, for the fossils, the integrity of the basic units of crocodylomorph eggshells and the bone microstructure were also observed.

2.3. THg analysis

Tooth samples were treated with nitric acid (10 %) for 10 s, followed by at least three separate rinses in 18.2 MΩ of deionized water for 24 h. Bone samples were equally processed, but they were not treated with nitric acid because they are more porous and, consequently, more sensitive to acid changes.

Nitric acid (HNO_3) was used because it efficiently oxidizes residual organic matter that could retain or release mercury during analysis and dissolves adsorbed or metallic Hg from surfaces. Therefore, it minimizes background contamination under “blank-limited” conditions and prevents cross-contamination between samples, improving analytical

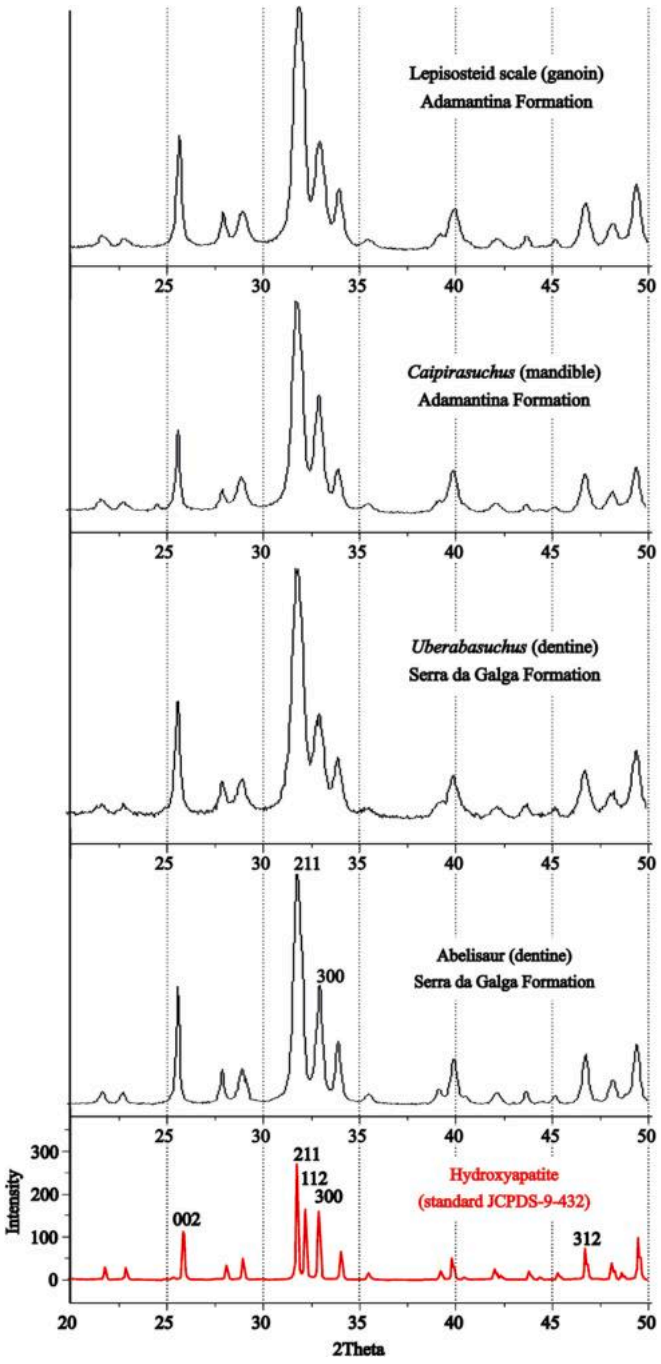

Fig. 1. X-ray diffraction of different bioapatite tissues (enamel, dentine, and bone cortex) from Adamantina and Serra da Galga formations in comparison with hydroxyapatite JCPDS-9-432 standard. Note that different tissues from different geological units have the same pattern, with peaks matching the standard material. A slightly broadening of all peaks is expected under exposure to low temperatures (~100 °C) with the formation of a CaO phase with additional planes (111), (200), and (220) (Indrani et al., 2017).

accuracy and reproducibility (Crock, 2005).

All the samples were air-dried at room temperature for 24 h and ground to a very fine homogeneous powder with an agate mortar. This ensured that the samples remained in contact with only amorphous SiO_2, a material with a high melting temperature that is not affected by subsequent pyrolysis during spectrophotometric analysis.

The samples of biomineralized fossil tissues and their host sediments were analyzed in triplicate aliquots of 200 mg each using Zeeman atomic absorption spectrometry at the Laboratory of Analytical and Environmental Chemistry of the University of Brasília. The analysis was conducted using a Lumeman® Portable Luminescence Zeeman Analyser RA 915+ (Lumex), being subjected to pyrolysis at temperatures ranging from 750 to 800 °C for 60 s.

Due to the absence of reference material for THg analyses in fossil mineralized bone, we used the SRM 1400 (bone ash) reference material from the National Institute of Standards and Technology (NIST), USA, to establish a preliminary analytical curve for THg concentration. The SRM 1400 is a suitable reference material because it best represents the structure found in fossil bioapatite. As SRM 1400 is produced by high temperature calcination, it does not contain mercury.

Before the analysis of the bone ash reference material, an analytical curve was generated to correlate the absorbance signal with known mercury concentrations (2, 5, 10, 20, 50, 100, and 150 $ng.g^{-1}$) by diluting a standard mercury solution of 1000 μg/ml (from Aldrich Chemical Company Inc.). The analyses were carried out under the following conditions: preheating time of 60 s, pyrolysis temperature set at 800 °C (module 1), analysis interval of 60 s, and aliquot volume of 200 μl to construct the calibration curve.

Following multiple reliable sources (e.g., WHO Expert Committee on Specifications for Pharmaceutical Preparations, 1992; Eurachem, 1998; ISO/IEC, 1999; US-FDA, F, 2001), we tested and validated key parameters, including the detection limit, range, recovery, calibration curve, linearity, and precision. The quality of measurements conducted by the Lumex 915+ was evaluated with recovery tests on enriched SRM 1400 reference material.

For SRM 1400 enrichment, the Hg standard solution (1000 μg/ml) from Aldrich Chemical Company Inc. was used. The accuracy of enriched concentrations (10, 25, and 60 $ng.g^{-1}$) yielded a recovery factor of 106.86 %, with a standard deviation of 4.20 for triplicate measurements. This indicates that associated errors are not statistically significant, ensuring reliable results without interference from other components in the measured analyte signal; for further details, see Cardia et al. (2018) and Supplementary Information 2.

2.4. Statistical analysis

To evaluate putative differences in THg concentrations among taxa and tissue types (bones and teeth), linear mixed-effects models (LMMs) were performed using the package *lme4* in R. The "full model" considered the columns *TissueType* and *Taxon* as fixed factors and *SiteLocation* as a random effect to evaluate potential non-independence among samples collected from the same geological unit. This analysis tested whether the type of fossil tissue and the taxonomic group significantly influenced THg values, whereas controlling for variation among sampling sites (geological unit).

A second model was evaluated after excluding rock sample values to focus exclusively on biological tissues (if THg concentration in bone and tooth enamel differs significantly) and to assess patterns of bioaccumulation in different taxa (see supplementary information files 3 and 4 for the data file and the script used in R, respectively). We performed an additional analysis excluding three juvenile specimens (two baurusuchids and one sphagesaurid) to evaluate the putative impact of ontogenetic dietary shifts on THg patterns within these groups.

The fixed-effect parameter estimates exhibit substantial covariance (see correlation matrix, Supplementary Information 5). This is expected with reference coding (intercept = Abelisauridae bones) and uneven sample sizes across taxa. Therefore, we used the adjusted marginal means (*emmeans*) and Tukey contrasts, which better account for parameter covariance and provide more robust pairwise comparisons among tissue types and taxa.

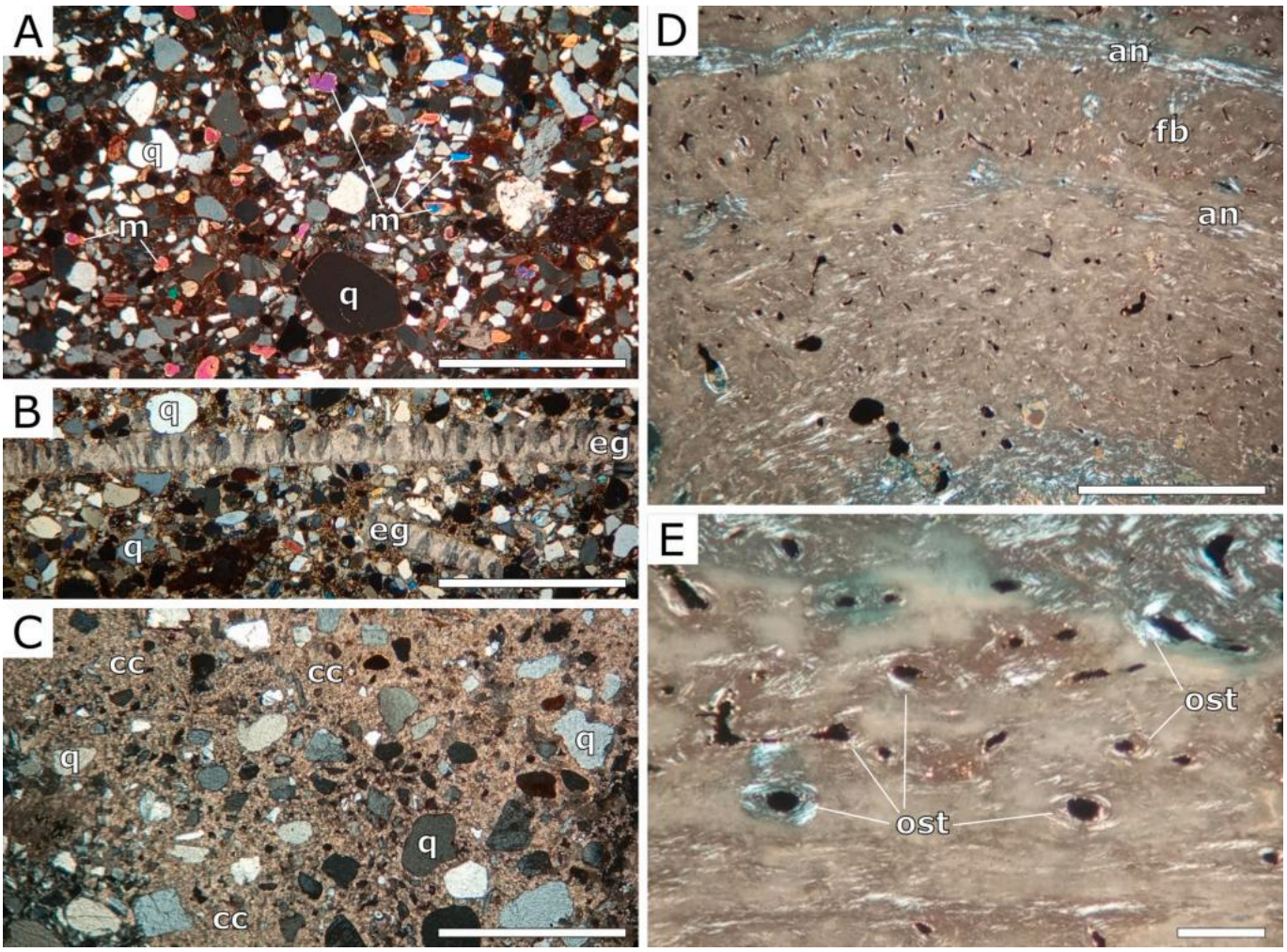

Fig. 2. Thin sections of different samples from the Bauru Group under polarized light. A-C, sandstones. D-E, fossil bone (cortex upward). A, Adamantina Formation sandstone. Note the quartz and mica grains showing well defined margins with no signs of dissolution or recrystallization. B, Adamantina Formation sandstone with crocodylomorph eggshell. The eggshell calcite crystals of the basic units show the original undulating extinction pattern. C, Marília Formation (Echaporã Member) sandstone with carbonate cement. D, baurusuchid long bone from the Adamantina Formation showing the original microstructure with some annuli composed of lamellar bone. E, magnification of the same thin section depicted in D showing osteons with the original microstructure. Abbreviations: an, annuli; cc, calcium carbonate cement, eg, eggshell; fb, fibrolamellar bone; m, mica; ost, osteon; q, quartz. Scale bars equal 1 mm in A-D, and 0.1 mm in E.

3. Results

3.1. Fossil preservation state and diagenetic alteration

Although commonly disarticulated, vertebrate fossils from the Bauru Group are generally well preserved. Previous studies have shown that teeth and bone tissue preserve their original hydroxyapatite microstructure (e.g., cyclical growth marks, Haversian system, and primary and secondary osteons) and that their crystallites have the expected size (e.g. Klock et al., 2022; Oliveira et al., 2021; Ricart et al., 2021; Muniz et al., 2025).

Fig. 1 presents X-ray diffraction patterns from various fossilized tissues (scales, teeth, and bones) collected from the Bauru Group (Adamantina and Serra da Galga formations), compared to the standard reference (International Centre for Diffraction Data, Powder Diffraction File 09–0432).

Notably, tissues such as ganoin from a lepisosteid fish scale and a bone sample from the crocodylomorph *Caipirasuchus* (Adamantina Formation), as well as dentine from *Uberabasuchus terrificus* and an abelisaurid (Serra da Galga Formation), exhibit diffraction peaks consistent with the fluorapatite standard material.

Furthermore, X-ray diffraction showed hydroxyapatite peaks with no significant shifts, broadening, and asymmetry, indicating that the crystallites were not affected by weathering or dissolution (e.g. Piga et al., 2011; Snyder et al., 2000) as also seen in other fossil samples from Bauru Group (e.g. Klock et al., 2022; Oliveira and Santucci, 2020; Oliveira et al., 2021).

The slight broadening of the diffraction peaks is expected in hydroxyapatite crystals subjected to low-temperature heating. Laboratory experiments with synthesized hydroxyapatite treated at different temperatures demonstrate that around 100 °C, the peaks broaden slightly and additional interference corresponding to the (111), (200), and (220) planes are present. This is consistent with the formation of a CaO phase with a mass fraction below 1 % (Indrani et al., 2017), which possibly obscures the peak associated with the (112) plane of hydroxyapatite (Fig. 1). At higher temperatures (900 °C), the peaks become sharper again and the CaO phase disappears (Indrani et al., 2017).

Thin sections of rocks and fossils from the Bauru Group (Fig. 2) provide additional evidence of minimal post-depositional alteration due to diagenesis. In sandstone samples, the sand fraction is primarily composed of unaltered primary minerals (quartz, feldspar, and micas) with no signs of recrystallization or dissolution, and exhibiting well-defined, regular grain boundaries. The same pattern is observed in the silt and clay fractions.

Whenever present, carbonate cement fills pore spaces with no signs of interactions with the primary minerals. Additionally, all sedimentary rock samples exhibit low or the lowest total mercury (THg) values of all sampled materials, including those cemented with $CaCO_3$. Calcium carbonate is known to act as a mercury sequestrant, since mercury can substitute for calcium in the Ca-carbonate bond as is seen in laboratory experiments and in soil analysis (e.g., Bilinski et al., 1980; Blais et al., 2008; Cho et al., 2021). This suggests that the rock matrix had originally relatively low THg concentrations and did not transfer mercury to the fossils.

Thin sections of fossil eggs and bones reveal well-preserved microstructures. The eggshells show clear calcite fibers with the expected size and optical properties, such as high-order interference colors, high relief, and undulating extinction patterns (Fig. 2 B). The bone microstructure also remains intact, with hydroxyapatite crystals of typical size, as well as the original configuration of woven and lamellar bone, including visible and well-defined growth lines. Primary and secondary osteons are well-preserved, along with smaller structures like osteocyte lacunae and their corresponding canaliculi (Fig. 2 D-E), suggesting that the samples were not significantly affected by post-depositional diagenetic alterations.

3.2. Hg concentrations

We analyzed a set of nearly 50 samples (fossils and rocks), comprising lepisosteiform fishes, anurans, testudines, notosuchian crocodyliforms, and non-avian theropod and sauropod dinosaurs, and birds, in some instances consisting of different ontogenetic stages (Table 1; SI 1).

The results consistently show higher values of THg in fossil biomineralized tissues than in their host rocks (Table 1, Figs. 3–4, SI 1), ranging from ca. 1.66 to 14.19 $ng.g^{-1}$ in fossil tissues, and from 0.00 to 5.75 $ng.g^{-1}$ in the sediments (mostly sandstones). In fact, THg concentration in rocks was uniformly low (ranging from 0.0 to 3.0 $ng.g^{-1}$), except for Adamantina Formation samples from particular areas (Table 1, Figs. 3–4), with values close to or slightly higher than 5.0 $ng.g^{-1}$.

Irrespective of the stratigraphic unit from which the fossils came, THg concentration is remarkably similar within the same vertebrate groups. Titanosaur fossil tissues, for example, have nearly constant and low (~ 4.5 $ng.g^{-1}$) THg values, whereas a much larger variation is seen in their host rocks (ranging from 0.0 to 5.3, see SI 1). Baurusuchidae crocodyliforms and abelisaurid theropods have the highest THg values (~from 10.0 to 14.0 $ng.g^{-1}$), whereas the lowest values are recorded for titanosaurs (~ 4.5 $ng.g^{-1}$).

Other crocodyliforms, such as peirosaurids (9.15 $ng.g^{-1}$), small- and large-sized sphagesaurids (~ 6.0 $ng.g^{-1}$), enantiornithine birds (5.71 $ng.g^{-1}$), and some Testudines (5.86 $ng.g^{-1}$), have intermediate THg values. Lepisosteiform fish (3.49 $ng.g^{-1}$), anurans (2.34 $ng.g^{-1}$), and some testudines, such as *Roxochelys* (1.72 $ng.g^{-1}$), showed the lowest THg values among the analyzed taxa.

We found significant differences in THg concentration for some crocodyliform (e.g., *Pisarrachampsa sera*, *Baurusuchus*, and *Caipirasuchus*), ranging from 17 % to 38 %, with adults being more enriched in THg (Table 1, SI 1). Among adult crocodyliform taxa (Table 1), the minimum and maximum values were respectively found for *Adamantinasuchus navae* (~3.0 $ng.g^{-1}$) and baurusuchids (~13.0 $ng.g^{-1}$), representing a difference of nearly 80 %.

Table 1
Example of THg in different Bauru Group taxa and rocks. THg values are given in $ng.g^{-1}$. Rock THg values were only measured when the respective fossil has at least a small amount of matrix attached to it. Abbreviations: Adam, Adamantina Formation; Ube, Uberaba Formation; Mar, Marília Formation; SG, Serra da Galga Formation; SD - standard deviation. * - refers to the taxa representing direct evidence of feeding habits in Baurusuchidae found in the Adamantina Formation. The raw data is available in SI 1.

Material	Clade	Type	Ontogenetic state	Unit (with THg values)	Collecting site	Mean	SD
Lepisosteidae	Lepisosteidae	scale	adult	Adam. Fm.	Presidente Prudente - SP	3.40	0.30
Baurubatrachus	Anura	bone	adult	Adam. Fm. (0.00)	Catanduva - SP	2.34	0.03
Turtle	Pleurodira	bone	adult	Adam. Fm. (5.36)	Presidente Prudente - SP	5.86	0.46
Roxochelys	Pleurodira	bone	adult	Adam. Fm. (0.98)	Monte Alto - SP	1.67	0.67
Morrinhosuchus	Sphagesauria	bone	adult	Adam. Fm.	Monte Alto - SP	3.18	1.47
Adamantinasuchus	Sphagesauridae	bone	adult	Adam. Fm.	Marília - SP	2.96	0.95
Mariliasuchus	Sphagesauria	tooth	adult	Adam. Fm. (2.42)	Marília - SP	5.23	0.77
Mariliasuchus	Sphagesauria	tooth	juvenile	Adam. Fm.	Marília - SP	2.71	0.69
Caipirasuchus	Sphagesauridae	bone	adult	Adam. Fm. (3.01)	Catanduva - SP	5.18	0.76
sphagesaurid*	Sphagesauridae	bone	adult	Adam. Fm. (5.30)	General Salgado - SP	6.59	2.18
sphagesaurid	Sphagesauridae	tooth	adult	Adam. Fm. (2.61)	Fernandópolis - SP	5.79	1.58
Caipirasuchus	Sphagesauridae	bone	juvenile	Adam. Fm.	Catanduva - SP	1.77	0.98
Caipirasuchus	Sphagesauridae	bone	adult	Adam. Fm. (2.92)	Monte Alto - SP	5.71	2.31
Itasuchus	Peirosauridae	tooth	adult	Adam. Fm.	Adamantina - SP	2.19	0.03
Montealtosuchus	Peirosauridae	bone	adult	Adam. Fm.	Monte Alto - SP	5.07	2.57
peirosaurid	Peirosauridae	tooth	adult	Adam. Fm.	Presidente Prudente - SP	9.15	2.70
*Aplestosuchus**	Baurusuchidae	bone	adult	Adam. Fm. (5.30)	General Salgado - SP	12.97	0.44
Pisarrachampsa	Baurusuchidae	bone	adult	Adam. Fm.	Gurinhatã - MG	5.11	0.06
Pisarrachampsa	Baurusuchidae	bone	juvenile	Adam. Fm.	Gurinhatã - MG	4.26	0.44
baurusuchid	Baurusuchidae	tooth	adult	Adam. Fm. (3.42)	Jales – SP	13.23	0.40
baurusuchid	Baurusuchidae	tooth	adult	Adam. Fm. (2.61)	Fernandópolis - SP	12.71	0.15
baurusuchid	Baurusuchidae	bone	adult	Adam. Fm.	Fernandópolis - SP	12.87	0.17
baurusuchid	Baurusuchidae	bone	juvenile	Adam. Fm.	Fernandópolis - SP	9.11	0.00
Aeolosaurus	Titanosauria	bone	adult	Adam. Fm.	Monte Alto - SP	4.35	0.15
titanosaur	Titanosauria	bone	adult	Adam. Fm.	Adamantina - SP	3.72	1.01
Brasilotitan	Titanosauria	bone	adult	Adam. Fm.	Presidente Prudente - SP	5.67	0.04
abelisaurid	Abelisauroidea	tooth	adult	Adam. Fm.	Adamantina - SP	13.16	1.65
abelissaurid	Abelisauroidea	tooth	adult	Adam. Fm.	Adamantina - SP	10.56	6.24
Bird	Enantiornithes	bone	unknown	Adam. Fm. (0.95)	Presidente Prudente - SP	5.71	2.32
Turtle	Pleurodira	bone	adult	Ube. Fm.	Uberaba - MG	1.38	0.15
titanosaur	Titanosauria	bone	adult	Ube. Fm. (0.39)	Uberaba - MG	4.45	1.81
titanosaur	Titanosauria	bone	adult	Mar. Fm.	Marília - SP	3.95	0.54
titanosaur	Titanosauria	bone	adult	Mar. Fm.	Monte Alto - SP	5.33	1.58
Itasuchus	Peirosauridae	tooth	adult	SG Fm. (0.00)	Uberaba - MG	2.36	0.22
titanosaur	Titanosauria	bone	adult	SG Fm.	Uberaba - MG	3.91	0.15

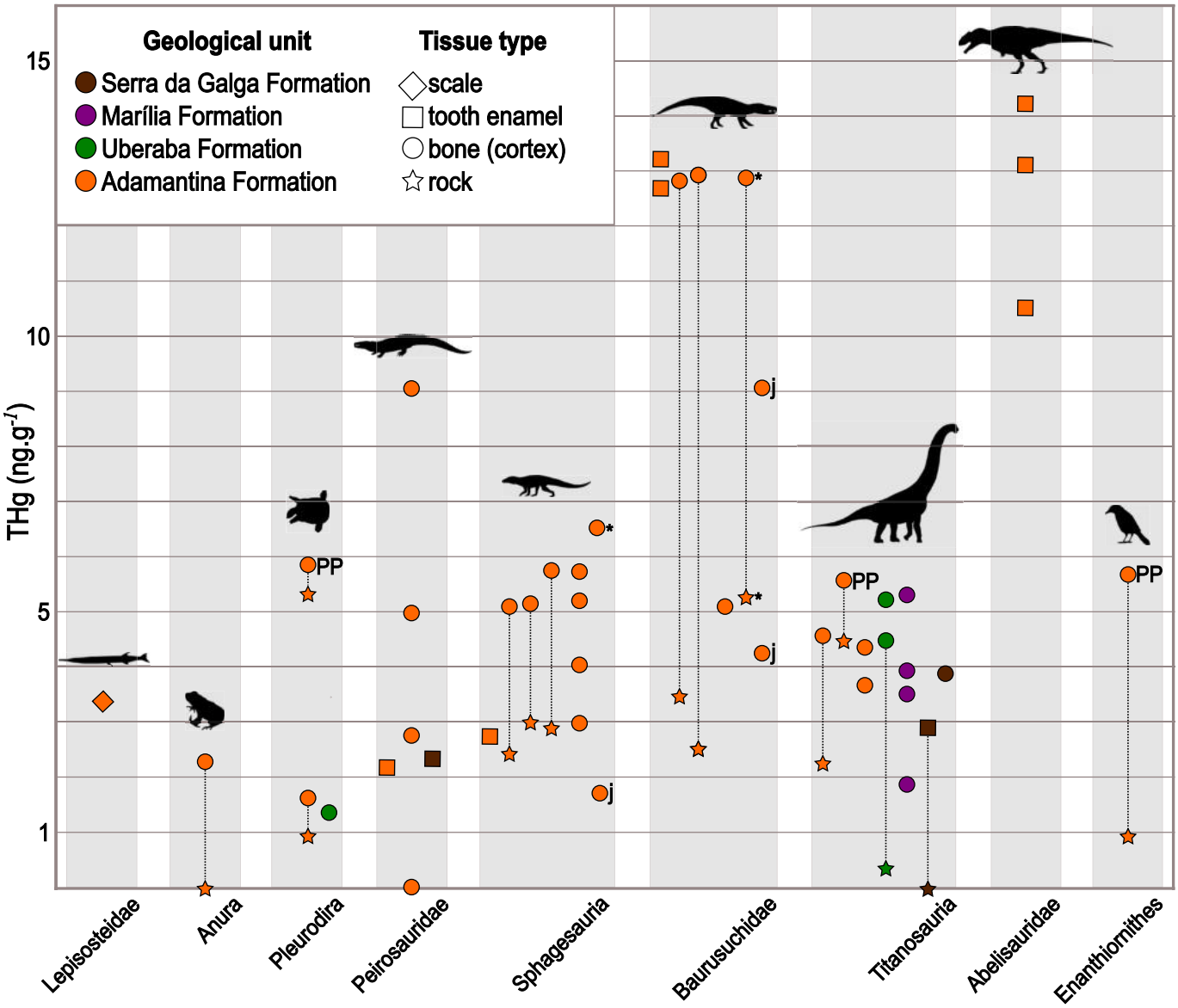

Fig. 3. Total Hg concentrations for different taxa, tissues, and geological units of the Bauru Group. Dashed lines connect rock samples analyzed in association with a specific fossil. PP, Presidente Prudente locality (fossils from this area exhibit relatively higher Hg concentrations); j, juvenile individuals; asterisks, *Aplestosuchus* (Baurusuchidae), sphagesaurid as stomachal content, and associated rock. The silhouettes are courtesy of http://phylopic.org/.

Data from a rare case of predation among fossil crocodyliforms, the baurusuchid *Aplestosuchus sordidus* with a sphagesaurid within its abdominal cavity (Godoy et al., 2014), showed the former with a THg concentration of 12.97 ng.g^{-1}, the sphagesaurid with 6.27 ng.g^{-1}, and the host rock with 5.30 ng.g^{-1}.

3.3. Statistical analysis

The Linear Mixed Model (LMM) evaluated patterns of Hg concentration in fossil tissues and taxa, considering geological unit as a random variation. In the complete model, rock samples were included as a "tissue type" to represent environmental background Hg, whereas the biological model excluded rocks (as a tissue type) to focus exclusively on fossilized tissues (Tables 2, 3, and Supplementary Information 5 for complete results from R command prompt).

The fit of the complete model (which considers rock samples as a tissue type) ranged from −2.15 to 2.24, with a mean of 0.04, indicating good symmetry and overall adequacy of the model (see Supplementary Information 5). The random effect associated with the geological unit (*SiteLocation*) showed a variance of 0.9457 and a standard deviation of 0.9725, suggesting a small variation in THg concentration among geological units. In contrast, the residual variance was 5.5508, with a standard deviation of 2.3560, indicating that THg concentration varies more among samples within the same geological unit than among different units. Regarding the fixed effects, rock samples exhibited, on average, 3.13 ng·g^{-1} less Hg than bone samples, with a significant *P*-value of 0.00014. The difference in Hg concentration between teeth and bones was 0.66 ng·g^{-1}, with a non-significant *P*-value of 0.5338 (see Supplementary Information 5).

The ANOVA results show a relatively high F value, indicating that both taxon and tissue type explain a significant portion of the variation in THg concentration values. Since this is a global test, the indication of differences among factor levels does not specify which levels differ from one another. In this case, using estimated marginal means (*emmeans*) allows the identification of which levels vary significantly. The adjusted values for rock samples are considerably lower than the estimated values for teeth and bones, whereas values for tooth and bone do not differ significantly (Table 2).

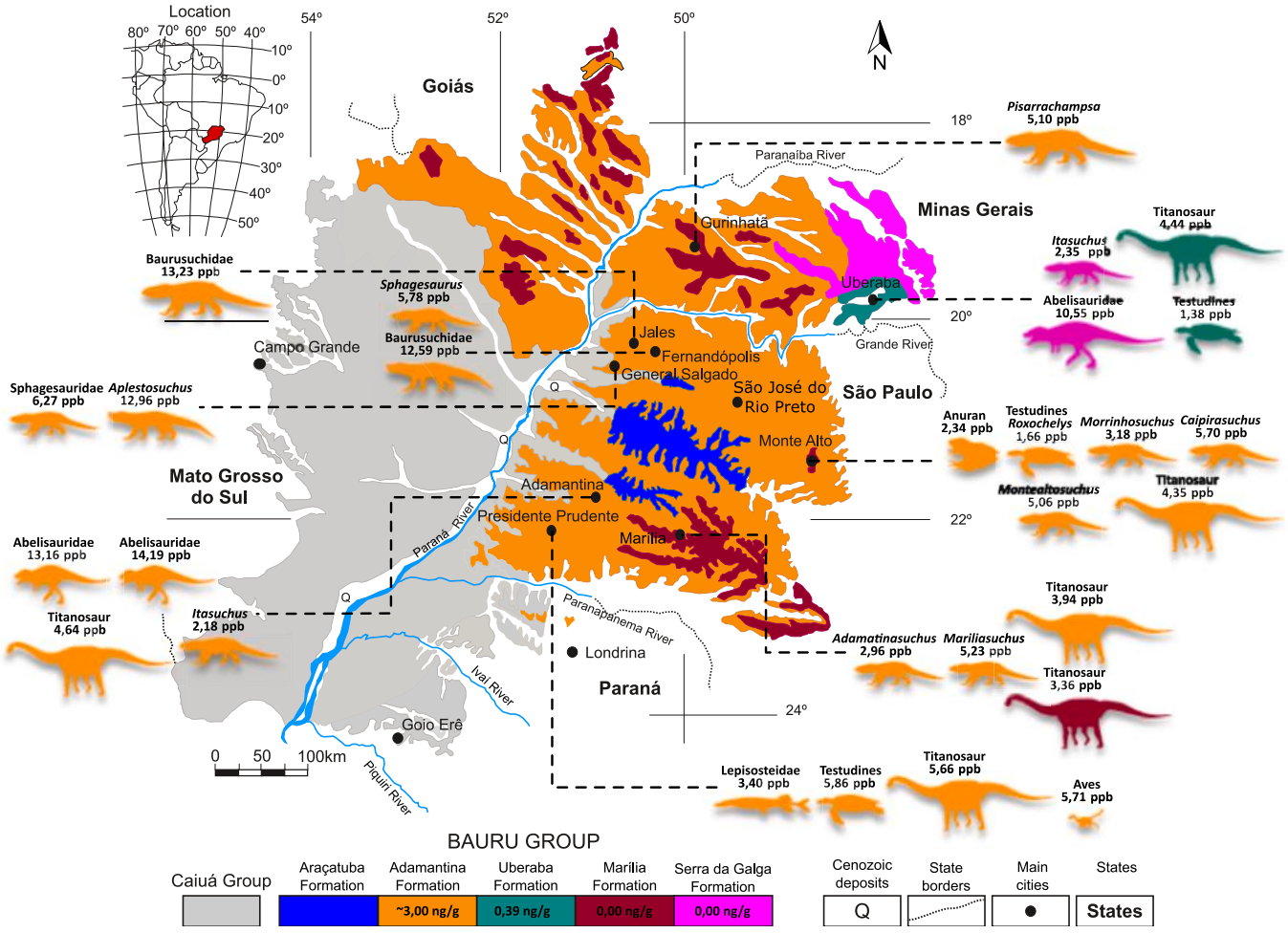

Fig. 4. Location and THg values of selected taxa from the Bauru Group. Silhouettes representing different taxa are not in scale. The color of taxa refers to the geological unit they were found (geological map modified from Fernandes and Coimbra, 2000; Tcacenco-Manzano and Fernandes, 2024). Mean rock THg values for each formation are provided in the key to the map.

Taxon explained substantial variation in Hg concentrations: Abelisauridae had the highest adjusted mean (10.27 ng.g^{-1}) and differed significantly from lower-trophic groups (e.g., Abelisauridae − Anura = 9.26 ng.g^{-1}, $p = 0.0079$; Abelisauridae − Peirosauridae = 8.13 ng.g^{-1}, $p = 0.0022$), consistent with trophic magnification (Table 2, Supplementary Information 5).

Similarly, the model that does not take rock Hg concentration in account ranged from −2.53 to 2.24, with a mean of 0.04, also indicating good symmetry and overall adequacy of the model (see Supplementary Information 5). The random effect (*SiteLocation*) is zero. Therefore, differences in Hg concentration among fossil tissues and taxa were not influenced by their geological unit, in contrast with the complete model (including rocks), where *SiteLocation* contributed in part to explain total variance.

The ANOVA results indicate that *TissueType* has no significant effect ($p = 0.91$), showing that bones and teeth exhibit statistically indistinguishable Hg concentrations. In contrast, *Taxon* shows a highly significant effect ($p < 0.001$), with a high F value (F = 8.83), confirming substantial differences among taxonomic groups. These results demonstrate that Hg variation among fossils is not dependent on tissue type but is clearly associated with taxonomic differences, reinforcing the hypothesis that Hg has a biological origin (bioaccumulation) rather than a taphonomic one (more related to geological context, Table 3).

Estimated marginal means (*emmeans*) show similar Hg concentrations in bones (5.77 ng.g^{-1}) and teeth (5.88 ng.g^{-1}; $p = 0.92$), indicating that tissue type did not influence Hg concentration, whereas taxonomic differences remained the dominant explanatory factor. This result further supports the interpretation that Hg distribution in fossil tissues reflects biological, rather than taphonomic, processes.

Pairwise comparisons of estimated marginal means for *Taxon* (averaged over *TissueType*) revealed marked differences in Hg concentration (Table 3, Supplementary Information 5). Abelisauridae showed the highest adjusted mean (12.6 ng.g^{-1}), significantly higher than Anura ($p = 0.034$), Peirosauridae (p = 0.002), Pleurodira ($p = 0.010$), and Sphagesauria (p = 0.002). No significant difference was observed between Abelisauridae and Baurusuchidae ($p = 0.93$), consistent with their similar carnivorous habits.

Taxa of lower trophic position (Anura, Pleurodira, Titanosauria) have significantly lower Hg values, indicating a strong trophic gradient in mercury bioaccumulation among Cretaceous vertebrates from the Bauru Group.

As ontogenetic differences in physiology and feeding behavior may impact within-taxon variance independently of taxonomic signals, a complementary linear mixed-effects model was run excluding juvenile specimens from the model with no rock samples to evaluate potential ontogenetic bias. Juveniles were unevenly distributed among taxa (two Baurusuchidae and one Sphagesauria), potentially influencing group means and variance estimates. In this case, the exclusion of juveniles did not alter the qualitative results of the model, but reduced residual variance and strengthened taxonomic contrasts, supporting the observed taxonomic signal (see Supplementary Information 5 for complete results).

Table 2
Main results of the linear mixed-effects model (LMM) analysis for the complete model, which includes THg concentrations in rock samples treated as a tissue type. NumDF = numerator degrees of freedom; DenDF = denominator degrees of freedom; SE standard error.

ANOVA (fixed effects)				
Factor	NumDF	DenDF	F value	*P* value
TissueType	2	48.55	9.56	0.00031
Taxon	7	44.61	7.18	9.444e^{-06}
Estimated marginal mean (THg) - *emmean* (tissue type)				
Tissue	*emmean*	SE	IC95% inf.	IC95% sup.
tooth	5.61	1.20	2.88	8.35
bone	4.96	1.08	1.48	8.43
rock	1.83	1.21	−1.39	5.05
Contrasts (Turkey)				
Comparison	Difference	P	Interpretation	
rock-tooth	−3.79	0.0073	tooth > rock	
rock-bone	3.13	0.0006	bone > rock	
tooth-bone	−0.66	0.82	tooth = bone	
Estimated marginal mean (THg) - *emmean* (taxon)				
Taxon	*emmean*	SE	IC95% inf.	IC95% sup.
Abelisauridae	10.27	1.94	6.25	14.28
Baurusuchidae	7.61	1.26	4,97	10.86
Enantiornithes	3.19	1.97	−0.82	7.20
Titanosauria	3.14	0,82	0,96	5,32
Sphagesauria	2.91	1.23	−0,43	6,26
Pleurodira	2.79	1.37	−0.13	5.71
Peirosauridae	2.14	1.41	−0.91	5.20
Anura	1.01	1.97	−3.00	5,02

Table 3
Main results of the linear mixed-effects model (LMM) analysis for the 'biological model' which excludes THg concentrations in rock samples. NumDF = numerator degrees of freedom; DenDF = denominator degrees of freedom; SE standard error.

ANOVA (fixed effects)				
Factor	NumDF	DenDF	F value	P value
TissueType	1	35.00	0.012	0.9118
Taxon	7	35.00	8.827	3.192e^{-06}
Estimated marginal mean (THg) - *emmean* (tissue type)				
Tissue	*emmean*	SE	IC95% inf.	IC95% sup.
tooth	5.88	1.36	1.84	9.93
bone	5.77	1.41	−90,424.00	90,435.00
Contrasts (Turkey)				
Comparison	Difference	P	Interpretation	
tooth-bone	−0.117	0.9194	tooth = bone	
Estimated marginal mean (THg) - *emmean* (taxon)				
Taxon	*emmean*	SE	IC95% inf.	IC95% sup.
Abelisauridae	12.58	2.23	6.61	18.54
Baurusuchidae	10.41	1.67	−11.69	8.12
Enantiornithes	5.77	2.80	0.046	11.49
Titanosauria	3.14	0,82	0.96	5.32
Sphagesauria	4.43	1.60	−68.99	77.85
Pleurodira	3.03	1.65	−0.41	6.47
Peirosauridae	4.19	0.83	2.27	6.10
Anura	2.40	2.80	−3.32	8.12

4. Discussion

4.1. The natural incorporation of Hg into bioapatite

The capacity of Hg to substitute Ca in bioapatite was discussed by Ávila et al. (2014) who, via EDS and X-ray diffractometry, found that some human teeth and bone samples from Mexico exhibited alterations in their hydroxyapatite lattice associated with Hg incorporation. In such case, the Hg substitution was identified because its ionic radius (0.127 nm) slightly exceeds that of Ca (0.114 nm), leading to an expansion of the unit cell parameters (Ávila et al., 2014).

Additionally, Cardia et al. (2018) first reported THg in vertebrate fossils (Baurusuchidae) from the Bauru Group (Upper Cretaceous), demonstrating that Hg can be trapped in fossil bones over long periods. In such study, similar THg concentrations were found in different tissues (tooth enamel and dentine, skull, axial, and appendicular bones), suggesting a biological rather than diagenetic origin of this element in such fossils.

Similarly, Meyer et al. (2019) found Hg in Cretaceous mollusk fossils, supporting the potential for Hg incorporation into biogenic mineralized tissues. As with bone hydroxyapatite, previous studies indicated that divalent metals like Hg with atomic radii comparable to that of calcium can substitute that element in the biogenic carbonate lattice (e.g., Jeffree et al., 1995; Yap et al., 2003; Brown et al., 2005).

Regarding mercury loss during diagenesis, Chen et al. (2022) and Liu et al. (2022) demonstrated that only minimal amounts of Hg are released under temperature and pressure intervals of 200–500C and 0.5–1.4 GPa, respectively, which are above the typical range of diagenetic conditions.

On the other hand, several studies demonstrate that the main elements incorporated into the bone during diagenesis are F, Fe, Mn, Si, Al, Sr, Ba, REE, Cl, and U (e.g. Kohn et al., 1999; Rogers et al., 2010; Herwartz et al., 2011, 2013; Piga et al., 2011; Keenan et al., 2015) either by alterations of the Ca and OH sites of bone hydroxyapatite or due to contamination by small-sized diagenetic minerals. Additionally, the stability constants (log K) for Hg–carbonate and Hg–phosphate complexes are considerably lower than those for Hg–sulfur or Hg–thiol ligands (Ravichandran, 2004), implying that Hg has only modest affinity with sulfur and dissolved organic matter under oxidizing diagenetic conditions like that found in Bauru Group deposits.

The THg concentrations measured in distinct biomineralized tissues (compact bone and dental enamel) further argue against diagenetic uptake, which would be expected to affect these tissues differentially. In addition, the significantly lower Hg concentrations in the host sandstones relative to the fossils indicate that the surrounding sediment did not serve as a substantial Hg reservoir. Collectively, these observations, combined with the chemical constraints implied by the log K values, suggest that diagenetic contamination is an unlikely source of the Hg measured in the fossils.

Additionally, cases of diagenetic Hg incorporation like fossil mammal bones and teeth from Late Miocene deposits in Spain (García-Alix et al., 2013) show that bone tissues are more enriched in Hg than dentine and tooth enamel because pores are generally larger and more abundant in bones. In this case, the fossils have a red color resulting from the diagenetic incorporation of cinnabar (HgS) in the tooth and bone pores (García-Alix et al., 2013).

Cinnabar has never been reported in Bauru Group rocks, neither in thin sections (Fig. 2) nor in X-ray diffraction analyses (Klock et al., 2022; Oliveira and Santucci, 2020; Oliveira et al., 2021). Moreover, in the present study, only dental enamel and cortical bone tissue were analyzed. The rocks of the Bauru Group, in which the sampled fossils were found, are predominantly sandstones, which are generally more porous than the analyzed tissues (see Fig. 2). Under a scenario of diagenetic Hg contamination, concentrations would be expected to be highest in the surrounding rocks, followed by bone tissue, and lowest in dental enamel.

Moreover, fossils from distinct taxa would be expected to have similar Hg concentrations, irrespective of their dietary habits. Neither of these patterns are observed in our results. Also, a previous analysis of THg in adult baurusuchids from the Bauru Group showed that their bone matrix and tooth enamel have similar values (~12.7–13.2 ng.g^{-1}, in some instances, the difference is less than 5 %), whereas the rock matrix has significatively lower THg values (~2.6–3.4 ng.g^{-1}), indicating that the fossil material did not undergo diagenetic alterations (Cardia et al., 2018).

Thus, considering the known natural processes of Hg incorporation into carbonate and bioapatite, as well as the effects of diagenesis on fossils, Hg analysis should be conducted with caution. Processes such as the incorporation of cinnabar (or other Hg-bearing minerals) and calcium carbonate, where Ca ions may be replaced by Hg, can alter the

original Hg composition of the sample.

In the case of the samples analyzed in this study, it is important to highlight that: (i) cinnabar is not observed in the examined rocks; (ii) carbonate cement in some rocks does not exhibit anomalous Hg concentrations (e.g., rocks with more carbonate cement do not contain more Hg than rocks with no carbonate); and (iii) similarly to archaeological studies on the natural presence of Hg in bone bioapatite (e.g., Cervini-Silva et al., 2013; Rasmussen et al., 2013; Emslie et al., 2015, 2019, 2022), the total Hg content in rocks from different units of the Bauru Group is generally significantly lower than those found in the studied fossils. Therefore, neither sediment composition nor diagenetic processes can account for the elevated Hg levels observed in the fossil material.

4.2. The Hg in fossil vertebrates of the Bauru Group

An important consideration when comparing Hg data among different specimens and taxa is that Hg concentrations in organism tissues from a given region are influenced by the amount of bioavailable Hg in the area. As noted earlier, Hg content in mussel shell carbonates from North Folk River, Virginia (USA), impacted by metal pollution varies according to the collection site, ranging, for example, from a mean of 8 ng.g^{-1} upstream of a pollution source to 387 ng.g^{-1} in areas of the same river affected by that Hg source. Low Hg values were observed in shell specimens collected prior to the installation of the pollution source (Brown et al., 2005).

A similar pattern has been observed in Hg analyses of recent bone tissue, although it is not clear whether the collagen, which usually has higher Hg concentrations than bone tissue, was removed prior to analyses. For example, a study on Hg concentrations in white-toothed shrews from contaminated and uncontaminated localities in Spain (Sánchez-Chardi et al., 2007), in uncontaminated areas, young males (due to nursing) exhibited higher Hg concentrations than adults (1040 and 950 ng.g^{-1}, respectively), whereas in polluted regions, young males have lower Hg concentrations than adults (1790 and 5530 ng.g^{-1}, respectively). These findings demonstrate that Hg concentration is sensitive to the availability of this element within the system (Sánchez-Chardi et al., 2007). The same effect of lactation was observed in a study on Hg in the bones of Steller sea lions, in which young individuals exhibited THg values of 31.4 ng.g^{-1}, whereas adults showed only 7.9 ng.g^{-1} (Keenan et al., 2024).

Mercury concentrations reported for bone samples of extant predators indicate that this element is incorporated into bioapatite in detectable quantities across trophic levels. For example, Hg in bioapatite of the red (*Vulpes vulpes*) and Arctic (*Vulpes lagopus*) foxes ranged from 36 to 100 ng.g^{-1} and 17 to 25 ng.g^{-1}, respectively (Dainowski and Duffy, 2021). Similarly, Racero-Casarrubia et al. (2012) reported THg values ranging from 38.3 to 88.7 ng.g^{-1} in jaguar tooth samples from Colombia.

In aquatic vertebrates, Schneider et al. (2015) found THg values of 153 ng.g^{-1} in *Caiman crocodilus*, 80 ng.g^{-1} in *Melanosuchus niger*, 2 ng.g^{-1} in *Podocnemis expansa*, and 0.5 ng.g^{-1} in *Podocnemis unifilis*. Considering these observations, the THg values measured in fossil samples from the Bauru Group are comparable to those reported in modern organisms, indicating a similar magnitude of Hg incorporation in bioapatite and a comparable biomagnification pattern.

Our analysis of Bauru Group vertebrate samples indicates that abelisaurids and baurusuchids were the top predators of the fauna, with THg averaging between 10 and 14 ng.g^{-1}, and abelisaurids showing slightly higher THg values (Table 1, SI1). This fits their size and craniomandibular anatomy, which indicates that they preyed on medium to large terrestrial vertebrates. Considering their known geographic occurrence in Bauru Group deposits (Bandeira et al., 2018), Baurusuchidae remains are generally found together with few other vertebrate taxa, mostly sphagesaurid crocodyliforms. Similarly, the sites where theropod dinosaur remains are found with no significant transport generally lack baurusuchid occurrences, suggesting that these two groups did not commonly inhabit the same area and did not compete for the same food resources (Bandeira et al., 2018). On the other hand, with an average THg of ~9.0 ng.g^{-1}, peirosaurid crocodyliforms correspond to intermediate predators. Indeed, they are characterized by more heterodont dentition and dorsoventrally compressed rostrum, hinting to a more diverse diet when compared to Baurusuchidae (Carvalho et al., 2004; Pinheiro et al., 2023).

Total mercury concentrations for Baurusuchidae and Peirosauridae are also in line with the presence of undigested bone fragments in Baurusuchidae coprolites from the Adamantina Formation (Oliveira et al., 2021) and $\delta^{13}C$ stable isotope analyses of *Uberabasuchus terrificus* and *Campinasuchus dinizi* teeth, which indicate that they respectively feed on terrestrial and aquatic food items (Klock et al., 2022).

The average THg concentrations in Sphagesauridae crocodyliforms, including those of the *Caipirasuchus* group, are between ~5.0 and 6.0 ng.g-1. Sphagesaurids have a highly heterodont dentition, with wear facets on molariform teeth indicating that they could perform propalinal jaw movements (Iori and Carvalho, 2018; Ősi, 2014; Pol, 2003; Ricart et al., 2021). Coprolites attributed to large sphagesaurids have plant material within (Oliveira et al., 2021), showing they included plants in their diets. Yet, Sphagesauridae THg concentrations are not as low as those of the strictly herbivorous sauropod dinosaurs, indicating that they included other food items in their diet.

The THg values for enantiornithine birds are similar to those of sphagesaurids (~ 5.0 ng.g^{-1}), suggesting a mixed diet, which is not uncommon among birds. Rare stomach contents show that some enantiornithines feed on invertebrates (Sanz et al., 1996), but given the diversity of their skull morphology, which includes edentulous species, they probably have fed on a wider range of food items (O'Connor, 2019).

Other Crocodyliformes, such as *Morrinhosuchus luziae* and *Mariliasuchus amarali*, in addition to lepisosteid fishes, anurans, and some turtles (*Roxochelys wanderleyi*), have low THg concentrations (between ~1.5 and 5.0 ng.g^{-1}), indicating that they could have been either herbivores or omnivores (Table 1, SI 1). *Morrinhosuchus luziae* and *Mariliasuchus amarali* are relatively small crocodyliforms with heterodont dentition akin to those seen in Sphagesauridae (Andrade and Bertini, 2008; Iori and Carvalho, 2009), justifying the similar THg values in these taxa.

Considering all analyzed crocodyliforms (e.g., Baurusuchidae, Peirosauridae Sphagesauria), the difference in THg concentrations found in their biomineralized tissues, together with their morphological diversity, strongly supports the idea that they developed a certain degree of dietary niche partitioning. Additionally, as previously noted for Baurusuchidae (Cardia et al., 2018), THg values vary with ontogeny in other crocodyliforms, with differences of approximately 37 % in adult specimens of *Caipirasuchus* relative to the juveniles and 17 % in *Pisarrachampsa sera* (Table 1). This difference associated with growth points to changes in their dietary habits during ontogeny.

Extant Lepisosteidae mainly prey on smaller fishes, but some taxa also feed on invertebrates such as snails and crabs and even on plant material (Grande, 2010). Indeed, some fossil Lepisosteidae were considered to have fed on gastropods (Grande, 2010). The THg values found in the fossil Lepisosteidae from the Bauru Group are consistent with a diet that includes invertebrates. The same holds true for anurans and the pleurodiran (*Roxochelys wanderleyi*), as their THg values are consistent with extant forms that feed on different invertebrates and sporadically on plants (Bour, 2007; Duellman and Trueb, 1994; Lemell et al., 2019; Solé and Rödder, 2010).

Several lines of evidence, such as dentition and coprolite content, indicate that titanosaurid sauropods are herbivores feeding on a relatively large array of plants (Oliveira and Santucci, 2020; Prasad et al., 2005), what could explain their variable, although generally low, THg values between ~2.0 and 4.5 ng.g^{-1}.

The THg values recovered for the only direct evidence of predation among Bauru Group crocodyliforms (Godoy et al., 2014) has the

predator (*Aplestosuchus sordidus*) with over 50.0 % more THg than the prey (a sphagesaurid) in its abdominal cavity, further validating the technique employed here (Table 1, Supplementary Information 1).

From the statistical point of view, the random effect of the geological unit (*SiteLocation*) exhibited near-zero variance, indicating that Hg concentrations in fossil tissues are mainly independent of the unit from which they were sampled. On the other hand, tissue type significantly influenced Hg values when rocks were included ($F = 9.56$, $p < 0.001$). Bones (*emmean* = 4.96 $ng.g^{-1}$) and teeth (mean = 5.61 $ng.g^{-1}$) contained higher Hg than surrounding rocks (mean = 1.83 $ng.g^{-1}$), whereas no significant difference was observed between bones and teeth ($p = 0.82$). If the Hg values of rocks are excluded, tissue type is non-significant, confirming comparable Hg accumulation across different fossil tissues. These results indicate that Hg enrichment in fossils cannot be attributed to the effect of surrounding matrix (Tables 2 and 3, Supplementary Information 5).

Taxonomic identity strongly affected Hg concentration in both models. Carnivorous taxa, particularly Abelisauridae and Baurusuchidae, exhibited the highest Hg values, whereas herbivorous (Titanosauria) and semi-aquatic taxa (Pleurodira, Anura) showed lower Hg concentrations. This pattern persisted even when Hg values from rocks are excluded, which is consistent with trophic-level biomagnification of Hg.

The fossil tissues are enriched in Hg relative to surrounding rocks, with similar THg concentrations in bones and teeth and significantly related to the taxonomic group of the sample. Together, these results suggest that Hg accumulation was primarily driven by trophic level rather than local sedimentary conditions, supporting long-term biogeochemical persistence and bioaccumulation of mercury through Mesozoic food webs.

5. Conclusions

Fossil vertebrate samples from the Bauru Group show Hg concentrations significantly higher than those in the host rocks, indicating that neither sediment composition nor diagenetic processes account for their THg elevated values. Additionally, these THg levels in Bauru Group fossils are comparable to those in modern biotas, suggesting a similar magnitude of incorporation into bioapatite and equivalent biomagnification patterns.

The trophic hierarchy of the Bauru Group vertebrates was reconstructed based on the THg concentration in mineralized tissues (bones and teeth). Distinct taxa were positioned at different trophic levels, such as top predators, intermediate consumers, and primary consumers (Fig. 5). This places abelisaurids and baurusuchids as top predators, peirosaurids as intermediate predators, and other taxa, including sphagesaurids, enantiornithine birds, and smaller crocodyliforms, at lower trophic levels. Herbivorous taxa such as titanosaurid sauropods exhibit generally low Hg values. The lower THg values observed in sphagesaurids also reinforce evidence found in their coprolites that this group of crocodylomorphs were herbivorous. Differences in THg between juvenile and adult individuals of the same species can be used as evidence for shifts in their feeding behavior.

The Hg analysis requires a small amount of material to be implemented and can be applied in other vertebrate-bearing deposits that did not undergo significant diagenetic alteration. However, this approach in fossil material must exclude diagenetic contamination (e.g., cinnabar impregnation, carbonate cementation), which can artificially elevate their Hg concentrations.

Declaration of AI use

We have not used AI-assisted technologies in creating this article.

CRediT authorship contribution statement

Felipe M.S. Cardia: Visualization, Validation, Methodology, Investigation, Formal analysis, Data curation, Conceptualization, Writing – review & editing, Writing – original draft. **José Vicente E. Bernardi:** Visualization, Supervision, Project administration, Methodology, Funding acquisition, Formal analysis, Conceptualization, Writing – review & editing. **Carlos Eduardo M. Oliveira:** Validation, Resources, Investigation, Data curation, Writing – review & editing. **Marco B. Andrade:** Validation, Resources, Investigation, Data curation, Writing –

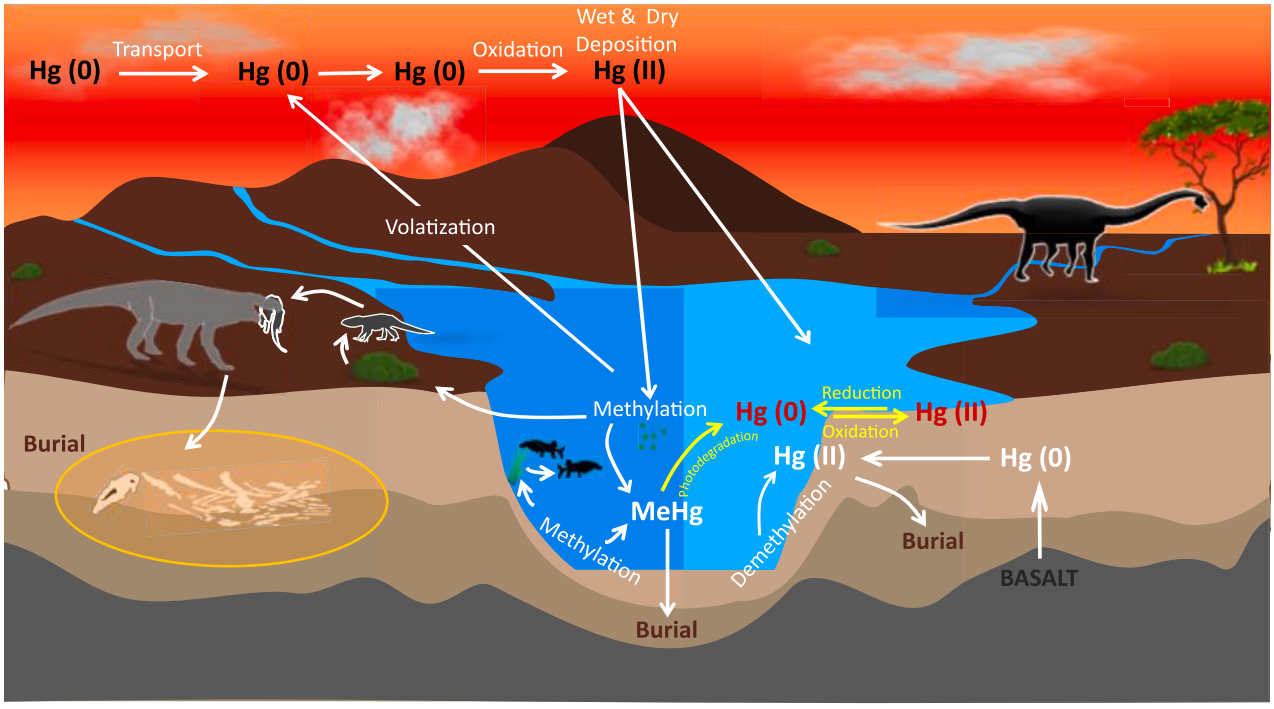

Fig. 5. Proposed Hg cycle for the Bauru Group and the process of Hg methylation and its incorporation along the trophic levels. Based on Selin (2009).

review & editing. **Max C. Langer:** Visualization, Resources, Data curation, Writing – review & editing. **Sandra A.S. Tavares:** Validation, Resources, Formal analysis, Writing – review & editing. **Fabiano V. Iori:** Validation, Resources, Data curation, Writing – review & editing. **William R. Nava:** Validation, Resources, Data curation, Writing – review & editing. **Thiago S. Marinho:** Validation, Resources, Data curation, Writing – review & editing. **Luiz Carlos B. Ribeiro:** Validation, Resources, Data curation, Writing – review & editing. **Jurandir R. Souza:** Validation, Resources, Methodology, Writing – review & editing. **Rodrigo M. Santucci:** Validation, Supervision, Resources, Investigation, Funding acquisition, Formal analysis, Data curation, Conceptualization, Writing – review & editing.

Declaration of competing interest

The authors declare that they have no known competing financial interests or personal relationships that could have appeared to influence the work reported in this paper.

Acknowledgements

This study was funded by the Coordenação de Aperfeiçoamento de Pessoal de Nível Superior – Brazil (CAPES) – Finance Code 001 (FMSC, JVEB, and RMS), CNPq (grants 401784/2010-0 and 311849/2014-8 to RMS, and grant 308900/2021-9 to TSM), and FAPESP (grant 20/07997-4 to MCL). We thank Lourdes Morais (IBRAM), Geraldo Martins (CAESB), and João Victor (TQB) for their assistance with the Hg analyses. We also thank José Garrofe Dórea (in memoriam) for his guidance during all stages of development of this work. The silhouettes used in Fig. 3 are courtesy of http://phylopic.org/. We are deeply grateful to Vasileios Mavromatis (Editor) and the two anonymous reviewers for their comments, which substantially improved an earlier version of this manuscript.

Appendix A. Supplementary data

Supplementary data to this article can be found online at https://doi.org/10.1016/j.chemgeo.2025.123218.

Data availability

The raw data of THg analyses are provided at Supplementary Informations 1 to 5.

References

Aksentov, K.I., Astakhov, A.S., Ivanov, M.V., Shi, X., Hu, L., Alatortsev, A.V., Sattarova, V.V., Mariash, A.A., Melgunov, M.S., 2021. Assessment of mercury levels in modern sediments of the East Siberian. Sea. Mar. Pollut. Bull. 168, 112426. https://doi.org/10.1016/j.marpolbul.2021.112.

Almli, B., Mwase, M., Sivertsen, T., Musonda, M., Flåøyen, A., 2005. Hepatic and renal concentrations of 10 trace elements in crocodiles (*Crocodylus niloticus*) in the Kafue and Luangwa rivers in Zambia. Sci. Total Environ. 337, 75–82.

Ambrose, S.H., Krigbaum, J., 2003. Bone chemistry and bioarchaeology. J. Anthropol. Archaeol. 22, 193–199.

Andrade, M.B., Bertini, R.J., 2008. Morphology of the dental carinae in *Mariliasuchus amarali* (Crocodylomorpha, Notosuchia) and the pattern of tooth serration among basal Mesoeucrocodylia. Arq. Mus. Nac. 66, 63–82.

Atwell, L., Hobson, K.A., Welch, H.E., 1998. Biomagnification and bioaccumulation of mercury in an arctic marine food web: insights from stable nitrogen isotope analysis. Can. J. Fish. Aquat. Sci. 55, 1114–1121.

Avery, J.P., Castellini, J.M., Misarti, N., Keenan, M., Gastaldi, A., Funk, C., O'Hara, T.M., Rea, L.D., 2023. Evaluating methods for determining mercury concentrations in ancient marine fish and mammal bones as an approach to assessing millennial-scale fluctuations in marine ecosystems. Front. Ecol. Evol. 11, 1251282. https://doi.org/10.3389/fevo.2023.1251282.

Ávila, A.P., Mansilla, J., Bosch, P., Pijoan, C., 2014. Cinnabar in Mesoamerica: poisoning or mortuary ritual? J. Archaeol. Sci. 49, 48–56.

Bandeira, K.L.N., Brum, A.S., Pêgas, R.V., Cidade, G.M., Holgado, B., Cidade, A., Souza, R.G., 2018. The Baurusuchidae vs Theropoda record in the Bauru Group (Upper cretaceous, Brazil): a taphonomic perspective. J. Iber. Geol. 44, 25–54.

Batezelli, A., 2017. Continental systems tracts of the Brazilian cretaceous Bauru Basin and their relationship with the tectonic and climatic evolution of South America. Basin Res. 29, 1–25.

Bergquist, B.A., 2017. Mercury, volcanism, and mass extinctions. PNAS 114, 8675–8677.

Bertini, R.J., Marshall, L.G., Gayet, M., Brito, P.M., 1993. Vertebrate faunas from the Adamantina and Marília (Upper Bauru Group, late cretaceous, Brazil) in their stratigraphic and paleobiogeographic context. Neues Jahrb. für Geol. und Paläontol., Monatshefte 188, 71–101.

Bilinski, H., Marković, M., Gessner, M., 1980. Solubility and equilibrium constants of mercury(II) in carbonate solutions (25 °C, I = 0.5 mol dm^{-3}). Inorg. Chem. 19 (11), 3440–3443.

Blais, J.F., Djedidi, Z., Ben Cheikh, R., Tyagi, R.D., Mercier, G., 2008. Metals precipitation from effluents: review. Pract. Period. Hazard. Toxic Radioact. Waste Manag. 12 (3), 135–149.

Bour, R., 2007. Global diversity of turtles (Chelonii; Reptilia) in freshwater. In: Balian, E. V., Lévêque, C., Segers, H., Martens, K. (Eds.), Freshwater Animal Diversity Assessment. Developments in Hydrobiology 198. Springer, Dordrecht. https://doi.org/10.1007/978-1-4374-0208-2_57.

Bourgon, N., Jaouen, K., Bacon, A.M., Dufour, E., McCormack, J., Tran, N.H., Trost, M., Fiorillo, D., Dunn, T.E., Zanolli, C., Zachwieja, A., Duringer, P., Ponche, J.L., Boesch, Q., Antoine, P.O., Westaway, K.E., Joannes-Boyau, R., Suzzoni, E., Frangeul, S., Crozier, F., Aubaile, F., Patole-Edoumba, E., Luangkhoth, T., Souksavatdy, V., Boualaphane, S., Sayavonkhamdy, T., Sichanthongtip, P., Sihanam, D., Demeter, F., Shackelford, L.L., Hublin, J.J., Tütken, T., 2021. Trophic ecology of a late Pleistocene early modern human from tropical Southeast Asia inferred from zinc isotopes. J. Hum. Evol. 161, 103075. https://doi.org/10.1016/j.jhevol.2021.103075.

Brown, M.E., Kowalewski, M., Neves, R.J., Cherry, D.S., Schreiber, M.E., 2005. Freshwater mussel shells as environmental chronicles: geochemical and taphonomic signatures of mercury-related extirpations in the North Fork Holston River, Virginia. Environ. Sci. Technol. 39 (6), 1455–1462.

Brown, C.M., Greenwood, D.R., Kalyniuk, J.E., Braman, D.R., Henderson, D.M., Greenwood, C.L., Basinger, J.F., 2020. Dietary palaeoecology of an early cretaceous armoured dinosaur (Ornithischia; Nodosauridae) based on floral analysis of stomach contents. R. Soc. Open Sci. 7, 200305.

Cardia, F.M.S., Santucci, R.M., Bernardi, J.V.E., Andrade, M.B., Oliveira, C.E.M., 2018. Mercury concentrations in terrestrial fossil vertebrates from the Bauru Group (Upper cretaceous), Brazil and implications for vertebrate paleontology. J. S. Am. Earth Sci. 86, 15–22.

Carvalho, I.S., Ribeiro, L.C.B., Avilla, L.S., 2004. *Uberabasuchus terrificus* sp. nov., a new Crocodylomorpha from the Bauru Basin (Upper cretaceous), Brazil. Gondwana Res. 7, 975–1002.

Castro, M.C., Goin, F.J., Ortiz-Jaureguizar, E., Vieytes, E.C., Tsukui, K., Ramezani, J., Batezelli, A., Marsola, J.C.A., Langer, M.C., 2018. A late cretaceous mammal from Brazil and the first radioisotopic age for the Bauru Group. R. Soc. Open Sci. 5180482. https://doi.org/10.1098/rsos.180482.

Cervini-Silva, J., et al., 2013. Cinnabar-preserved bone structures from primary osteogenesis and fungal signatures in ancient human remains. Geomicrobiol J. 30, 566–577.

Chen, D., Ren, D., Deng, C., Tian, Z., Yin, R., 2022. Mercury loss and isotope fractionation during high-pressure and high-temperature processing of sediments: implication for the behaviors of mercury during metamorphism. Geochim. Cosmochim. Acta 334, 231–240.

Chiappe, L.M., Navalón, G., Martinelli, A.G., Nava, W.R., Field, D.J., 2022. Fossil basicranium clarifies the origin of the avian central nervous system and inner ear. Proc. R. Soc. B 289, 20221398. https://doi.org/10.1098/rspb.2022.1398.

Cho, K., Kang, J., Kim, S., Purev, O., Myung, E., Kim, H., Choi, N., 2021. Effect of inorganic carbonate and organic matter in thermal treatment of mercury-contaminated soil. Environ. Sci. Pollut. Res. 28, 48184–48193.

Comans, C.M., Smart, S.M., Kast, E.R., Lu, Y., Lüdecke, T., Leichliter, J.N., Sigman, D.M., Ikejiri, T., Martínez-García, A., 2024. Enameloid-bound δ15N reveals large trophic separation among late cretaceous sharks in the northern Gulf of Mexico. Geobiology 22 (1), e12585. https://doi.org/10.1111/gbi.12585.

Crock, J.G., 2005. Determination of total mercury in biological and geological samples. In: U.S. Geological Survey Open-File Report 2005–1030, p. 59.

Dainowski, B.H., Duffy, L.K., 2021. A forensic evaluation: the use of mercury and stable isotope analysis of museum bone samples to monitor if environmental changes are affecting the eating patterns of red and Arctic foxes. Adv. Clin. Toxicol. 6, 1–9.

Delcourt, R., Brilhante, N.S., Pires-Domingues, R.A., Hendrickx, C., Grillo, O.N., Augusta, B.G., Maciel, B.S., Ghilardi, A.M., Ricardi-Branco, F., 2024. Biogeography of theropod dinosaurs during the late cretaceous: evidence from Central South America. Zool. J. Linnean Soc. zlad184.

Duellman, W.E., Trueb, L., 1994. Biology of Amphibians. John Hopkins University Press, Baltimore & London.

Emslie, S.D., Brasso, R., Patterson, W., Valera, A.C., McKenzie, A., Silva, A.M., Gleason, J. D., Blum, J.D., 2015. Chronic mercury exposure in late Neolithic/Chalcolithic populations in Portugal from the cultural use of cinnabar. Sci. Rep. 5. https://doi.org/10.1038/srep14679.

Emslie, S.D., Alderman, A., McKenzie, A., Brasso, R., Taylor, A., Molina Moreno, M., Cambra-Moo, O., Martin, A.G., Silva, A.M., Valera, A., Vijande Vila, E., 2019. Mercury in archaeological human bone: biogenic or diagenetic? J. Archaeol. Sci. 108, 104969. https://doi.org/10.1016/j.jas.2019.05.005.

Emslie, S.D., Silva, A.M., Valera, A., Vijande Vila, E., Melo, L., Curate, F., Fidalgo, D., Inacio, N., Molina Moreno, M., Cambra-Moo, O., Gonzalez Martin, A., Barroso-Bermejo, R., Montero Artus, R., Garcia Sanjuan, L., 2022. The use and abuse of

cinnabar in late Neolithic and Copper Age Iberia. Int. J. Osteoarchaeol. 32 (1), 202–214. https://doi.org/10.1002/oa.3056.
Eurachem, 1998. The fitness for purpose of analytical methods. In: Eurachem Guide. ISBN 0-454 94948 926-12-0. https://doi.org/978-91-87461-59-0.
Fernandes, L.A., Coimbra, A.M., 2000. Revisão estratigráfica da parte oriental da Bacia Bauru (Neocretáceo). Rev. Brasi. Geoci. 30, 717–728.
Font, E., Adatte, T., Sial, A.N., Lacerda, L.D., Keller, G., Punekar, J., 2016. Mercury anomaly, Deccan volcanism, and the end-cretaceous mass extinction. Geology 44, 171–174.
França, M.A.G., Langer, M.C., 2005. A new freshwater turtle (Reptilia, Pleurodira, Podocnemidae) from the Upper cretaceous (Maastrichtian) of Minas Gerais, Brazil. Geodiversitas 27, 391–411.
Fricke, H.C., 2007. Stable isotope geochemistry of bonebed fossils: Reconstructing paleoenvironments, paleoecology, and paleobiology. In: Bonebeds: Genesis, Analysis, and Paleobiological Significance. University of Chicago Press, Chicago, pp. 437–490.
García-Alix, A., Minwer-Barakat, R., Suárez, E.M., Freudenthal, M., Huertas, A.D., 2013. Cinnabar mineralization in fossil small mammal remains as a consequence of diagenetic processes. Lethaia 46, 1–6.
Godoy, P.L., Montefeltro, F.C., Norell, M.A., Langer, M.C., 2014. An additional baurusuchid from the cretaceous of Brazil with evidence of interspecific predation among Crocodyliformes. PLoS One 9, e97138.
Grande, L., 2010. An empirical synthetic pattern study of gars (Lepisosteiformes) and closely related species, based mostly on skeletal anatomy. Ichthyol. Herpetol. 10, 1–871.
Herwartz, D., Tütken, T., Münker, C., Jockum, K.P., Stool, B., Sander, P.M., 2011. Timescales and mechanisms of REE and Hf uptake in fossil bones. Geochim. Cosmochim. Acta 75, 82–105.
Herwartz, D., Tütken, T., Jockum, K.P., Sander, P.M., 2013. Rare earth element systematics of fossil bone revealed. Geochim. Cosmochim. Acta 103, 161–183.
Heuser, A., Tütken, T., Gussone, N., Galer, S.J.G., 2011. Calcium isotopes in fossil bones and teeth — Diagenetic versus biogenic origin. Geochim. Cosmochim. Acta 75, 3419–3433.
Indrani, D.J., Soegijono, B., Adi, W.A., Trout, N., 2017. Phase composition and crystallinity of hydroxyapatite with various heat treatment temperatures. Int. J. Appl. Pharma. 9 (Special Issue 2), 87–91.
Iori, F.V., Carvalho, I.S., 2009. *Morrinhosuchus luziae*, um novo Crocodylomorpha Notosuchia da Bacia Bauru, Brasil. Brazil. J. Geol. 39, 717–725.
Iori, F.V., Carvalho, I.S., 2018. The cretaceous crocodyliform *Caipirasuchus*: behavioral feeding mechanisms. Cretac. Res. 84, 181–187.
ISO/IEC, 1999. General Requirements for the Competence of Calibration and Testing Laboratories. ISO/IEC, 17025.
Jeffree, R.A., Markich, S.J., Brown, P.L., 1995. Australian freshwater bivalves: their applications in metal pollution studies. Aust. J. Ecotoxicol. 1, 33–41.
Jones, D.S., Martini, A.M., Fike, D.A., Kaiho, K., 2017. A volcanic trigger for the late Ordovician mass extinction? Mercury data from South China and Laurentia. Geology 45, 631–634.
Kast, E.R., Griffiths, M.L., Kim, S.L., Rao, Z.C., Shimada, K., Becker, M.A., Maisch, H.M., Eagle, R.A., Clarke, C.A., Neumann, A.N., Karnes, M.E., Lüdecke, T., Leichliter, J.N., Martínez-García, A., Akhtar, A.A., Wang, X.T., Haug, G.H., Sigman, D.M., 2022. Cenozoic megatooth sharks occupied extremely high trophic positions. Sci. Adv. 8 (25). https://doi.org/10.1126/sciadv.abl6529 eabl6529.
Keenan, S.W., Engel, A.S., Roy, A., Bovenkamp-Langlois, G.L., 2015. Evaluating the consequences of diagenesis and fossilization on bioapatite lattice structure and composition. Chem. Geol. 413, 18–27.
Keenan, M., Misarti, N., Horstmann, L., Crawford, S.G., O'Hara, T., Rea, L.D., Avery, J.P., 2024. Total mercury concentrations in Steller Sea lion bone: variability among locations and elements. Mar. Pollut. Bull. 203, 116471. https://doi.org/10.1016/j.marpolbul.2024.116471.
Klock, C., Leuzinger, L., Santucci, R.M., Martinelli, A.G., Marconato, A., Marinho, T.S., Luz, Z., Vennemann, T., 2022. A bone to pick: stable isotope compositions as tracers of food sources and paleoecology for notosuchians in the Brazilian Upper cretaceous Bauru Group. Cretac. Res. 131, 105113.
Koch, P.L., 2007. Isotopic study of the biology of modern and fossil vertebrates. In: Stable Isotopes in Ecology and Environmental Science. Blackwell Publishing Ltd, pp. 99–154.
Kohn, M.J., Schoeninger, M.J., Barker, W.W., 1999. Altered states: effects of diagenesis on fossil tooth chemistry. Geochim. Cosmochim. Acta 63, 2737–2747.
Kolodny, Y., Luz, B., Sander, M., Clemens, W.A., 1996. Dinosaur bones: fossils or pseudomorphs? The pitfalls of physiology reconstruction from apatitic fossils. Palaeogeogr. Palaeoclimatol. Palaeoecol. 126, 161–171.
Langer, M.C., Delcourt, R., Montefeltro, F.C., Silva Júnior, J.C., Soler, M.G., Ferreira, G. S., Ruiz, J.V., Barcelos, L.A., Onary, S., Marsola, J.C.A., Castro, M.C., Cidade, G.M., Batezelli, A., 2022. The Bauru Basin in São Paulo and its tetrapods. Derbyana 43, e776.
Lavoie, R.A., Jardine, T.D., Chumchal, M.M., Kidd, K.A., Campbell, L.M., 2013. Biomagnification of mercury in aquatic food webs: a worldwide meta-analysis. Environ. Sci. Technol. 47, 13385–13394.
Lemell, P., Natchev, N., Beisser, C.J., Heiss, E., 2019. Feeding in turtles: Understanding terrestrial and aquatic feeding in a diverse but monophyletic group. In: Bels, V., Whishaw, I. (Eds.), Feeding in Vertebrates. Fascinating Life Sciences. Springer (chapter 16).
Liu, Z., Tian, H., Yin, R., Chen, D., Gai, H., 2022. Mercury loss and isotope fractionation during thermal maturation of organic-rich mudrocks. Chem. Geol. 612, 121144.
Liu, M., Yuan, W., Fang, C., Wang, X., Tan, N., Zhao, M., Wang, X., Algeo, T.J., Sun, P., Feng, X., Chen, D., 2025. Mercury isotope evidence for Middle Ordovician photic-zone euxinia: implications for termination of the Great Ordovician biodiversification event. Gondwana Res. 137, 131–144.
Lüdecke, T., Leichliter, J.N., Stratford, D., Sigman, D.M., Vonhof, H., Haug, G.H., Bamford, M.K., Martínez-García, A., 2025. *Australopithecus* at Sterkfontein did not consume substantial mammalian meat. Science 387 (6731), 309–314.
Maisey, J.G., 1994. Predator-prey relationships and trophic level reconstruction in a fossil fish community. Environ. Biol. Fish 40, 1–22.
Martin, J.E., Tacail, T., Adnet, S., Girard, C., Balter, V., 2015. Calcium isotopes reveal the trophic position of extant and fossil elasmobranchs. Chem. Geol. 415, 118–125. https://doi.org/10.1016/j.chemgeo.2015.09.011.
Martin, J.E., Vincent, P., Tacail, T., Khaldoune, F., Jourani, E., Bardet, N., Balter, V., 2017. Calcium isotopic evidence for vulnerable marine ecosystem structure prior to the K/Pg extinction. Curr. Biol. 27 (11), 1641–1644.e2. https://doi.org/10.1016/j.cub.2017.04.043.
Martins, K.C., Queiroz, M.V.L., Ruiz, J.V., Langer, M.C., Montefeltro, F.C., 2024. A new Baurusuchidae (Notosuchia, Crocodyliformes) from the Adamantina Formation (Bauru Group, Upper cretaceous), with a revised phylogenetic analysis of Baurusuchia. Cretac. Res. 153, 105680.
Mason, R.P., Reinfelder, J.R., Morel, F.M.M., 1995. Bioaccumulation of mercury and methylmercury. Water Air Soil Pollut. 80, 915–921.
McCormack, J., Griffiths, M.L., Kim, S.L., Shimada, K., Karnes, M., Maisch, H., Pederzani, S., Bourgon, N., Jaouen, K., Becker, M.A., Jöns, N., Sisma-Ventura, G., Straube, N., Pollerspöck, J., Hublin, J.J., Eagle, R.A., Tütken, T., 2022. Trophic position of *Otodus megalodon* and great white sharks through time revealed by zinc isotopes. Nat. Commun. 13 (1), 2980. https://doi.org/10.1038/s41467-022-30528-9.
McCormack, J., Feichtinger, I., Fuller, B.T., Jaouen, K., Griffiths, M.L., Bourgon, N., Maisch, H., Becker, M.A., Pollerspöck, J., Hampe, O., Rössner, G.E., Assemat, A., Müller, W., Shimada, K., 2025. Miocene marine vertebrate trophic ecology reveals megatooth sharks as opportunistic supercarnivores. Earth Planet. Sci. Lett. 664, 119392. https://doi.org/10.1016/j.epsl.2025.119392.
Meloro, C., Hudson, A., Rook, L., 2015. Feeding habits of extant and fossil canids as determined by their skull geometry. J. Zool. 295, 178–188.
Meyer, K.W., Petersen, S.V., Lohmann, K.C., Blum, J.D., Washburn, S.J., Johnson, M.W., Gleason, J.D., Kurz, A.Y., Winkelstern, I.Z., 2019. Biogenic carbonate mercury and marine temperature records reveal global influence of Late Cretaceous Deccan Traps. Nat. Commun. 10, 5356. https://doi.org/10.1038/s41467-019-13366-0.
Michailow, M.M., Lugli, F., Cipriani, A., Della Giustina, F., Ferretti, A., Malferrari, D., Fowler, D., Fowler, E.F., Weber, M., Tütken, T., 2025. Combined Ca, Sr isotope and trace element analyses of Late Cretaceous dinosaur teeth: assessing diet versus diagenesis. Geochim. Cosmochim. Acta 400, 172–189. https://doi.org/10.1016/j.gca.2025.05.006.
Morel, F.M., Kraepiel, A.M., Amyot, M., 1998. The chemical cycle and bioaccumulation of mercury. Annu. Rev. Ecol. Syst. 29, 543–566.
Moubtahij, Z., McCormack, J., Bourgon, N., Trost, M., Sinet-Mathiot, V., Fuller, B.T., Smith, G.M., Temming, H., Steinbrenner, S., Hublin, J.J., Bouzouggar, A., Turner, E., Jaouen, K., 2024. Isotopic evidence of high reliance on plant food among later Stone Age hunter-gatherers at Taforalt, Morocco. Nat. Ecol. Evolut. 8 (5), 1035–1045.
Mulder, E.W.A., 2013. On the piscivorous behaviour of the early cretaceous amiiform neopterygian fish *Calamopleurus cylindricus* from the Santana Formation, Northeast Brazil. Neth. J. Geosci. 92, 119–122.
Muniz, F., Hsiou, A.S., de Andrade, F.D., Osés, G.L., Rizzutto, M., Pacheco, M.L.A.F., 2025. Diagenetic characterization of crocodyliform fossils from the Adamantina Formation (Upper cretaceous, Bauru Group): evaluating the chemical alteration of skeletal tissues through a multi-technique approach. Cretac. Res. 106248. https://doi.org/10.1016/j.cretres.2025.106248.
Nava, W.R., Martinelli, A.G., 2011. A new squamate lizard from the Upper cretaceous Adamantina Formation (Bauru Group), São Paulo State, Brazil. An. Acad. Bras. Cienc. 83, 291–299.
O'Connor, J.K., 2019. The trophic habits of early birds. Palaeogeogr. Palaeoclimatol. Palaeoecol. 513, 178–195.
O'Connor, J., Zhou, Z., Xu, X., 2011. Additional specimen of *Microraptor* provides unique evidence of dinosaurs preying on birds. PNAS 108, 19662–19665.
O'Keefe, F.R., Street, H.P., Cavigelli, J.P., Socha, J.J., O'Keefe, R.D., 2009. A plesiosaur containing an ichthyosaur embryo as stomach contents from the Sundance Formation of the Bighorn Basin, Wyoming. J. Vertebr. Paleontol. 29, 1306–1310.
Oliveira, F.A., Santucci, R.M., 2020. Palynological analysis of coprolites from the Marília Formation, Bauru Group (Upper cretaceous), Minas Gerais, Brazil. Cretac. Res. 115 (444), 104545.
Oliveira, F.A., Santucci, R.M., Oliveira, C.E.M., Andrade, M.B., 2021. Morphological and compositional analyses of coprolites from the Upper cretaceous Bauru Group reveal dietary habits of notosuchian fauna. Lethaia 54, 664–686.
Ősi, A., 2014. The evolution of jaw mechanism and dental function in heterodont crocodyliforms. Hist. Biol. 26, 279–414.
Percival, L.M.E., Ruhl, M., Hesselbo, S.P., Jenkyns, H.C., Mather, T.A., Whiteside, J.H., 2017. Mercury evidence for pulsed volcanism during the end-Triassic mass extinction. Proc. Natl. Acad. Sci. 114, 7929–7934.
Piga, G., Santos-Cubedo, A., Brunetti, A., Piccinini, M., Malgosa, A., Napolitano, E., Enzo, S., 2011. A multi-technique approach by XRD, XRF, FT-IR to characterize the diagenesis of dinosaur bones from Spain. Palaeogeogr. Palaeoclimatol. Palaeoecol. 310 (1–2), 92–107.
Pinheiro, A.E.P., Pereira, L.G.C., Vasconcellos, F.M., Brum, A.S., Souza, L.G., Costa, F.R., Castro, L.O.R., Silva, K.F., Bandeira, K.L.N., 2023. New *Itasuchidae* (Sebecia, Ziphosuchia) remains and the radiation of an elusive Mesoeucrocodylia clade. Hist. Biol. 35, 2280–2305.

Pol, D., 2003. New remains of *Sphagesaurus huenei* (Crocodylomorpha: Mesoeucrocodylia) from the late cretaceous of Brazil. J. Vertebr. Paleontol. 23 (4), 817–831.
Prasad, V., Stromberg, C.A., Alimohammadian, H., Sahni, A., 2005. Dinosaur coprolites and the early evolution of grasses and grazers. Science 310, 1177–1180.
Racero-Casarrubia, J.A., Marrugo-Negrete, J.L., Pinedo Hernández, J.J., 2012. Hallazgo de mercurio en piezas dentales de Jaguares (*Panthera onca*) provenientes de la zona amortiguadora del Parque Nacional Natural Paramillo, Córdoba, Colombia. RLC 2-3, 87–92.
Rasmussen, K.L., Skytte, L., Ramseyer, N., Boldsen, J.L., 2013. Mercury in soil surrounding medieval human skeletons. Herit. Sci. 1, 1–10.
Ravichandran, M., 2004. Interactions between mercury and dissolved organic matter—a review. Chemosphere 55, 319–331.
Ricart, R.S.D., Santucci, R.M., Andrade, M.B., Oliveira, C.E.M., Nava, W.R., Degrazia, G. F., 2021. Dental histology of three notosuchians (Crocodylomorpha) from the Bauru Group, Upper cretaceous, South-eastern Brazil. Hist. Biol. 33, 1012–1023.
Rogers, R.R., Fricke, H.C., Addona, V., Canavan, R.R., Dwyer, C.N., Harwood, C.L., Koenig, A.E., Murray, R., Thole, J.T., Williams, J., 2010. Using laser ablation-inductively coupled plasma-mass spectrometry (LA-ICP-MS) to explore geochemical taphonomy of vertebrate fossils in the Upper cretaceous two medicine and Judith River formations of Montana. Palaios 25 (3), 183–195.
Ruiz, J.V., Bronzati, M., Ferreira, G.S., Martins, K.C., Queiroz, M.V.L., Langer, M.C., Montefeltro, F.C., 2021. A new species of *Caipirasuchus* (Notosuchia, Sphagesauridae) from the late cretaceous of Brazil and the evolutionary history of Sphagesauria. J. Syst. Palaeontol. 19, 265–287.
Sánchez-Chardi, A., Lopez-Fuster, M.J., Nadal, J., 2007. Bioaccumulation of lead, mercury, and cadmium in the greater white-toothed shrew, *Crocidura russula*, from the Ebro Delta (NE Spain): sex- and age-dependent variation. Environ. Pollut. 145, 7–14.
Santos, I.R., Silva-Filho, E.V., Schaefer, C., Sella, S.M., Silva, C.A., Gomes, V., Passos, M. J., Van Ngan, P., 2006. Baseline mercury and zinc concentrations in terrestrial and coastal organisms of Admiralty Bay, Antarctica. Environ. Pollut. 140, 304–311.
Santos, R.O., Carvalho, A.B., Zaher, H., 2023. A new fossil frog (Lissamphibia: Anura) from the late cretaceous of Brazil and the early evolution of neobatrachians. Zool. J. Linnean Soc. zlad167.
Santucci, R.M., Filippi, L.S., 2022. Last titans: titanosaurs from the Campanian–Maastrichtian age. In: South American Sauropodomorph Dinosaurs: Record, Diversity and Evolution. Springer International Publishing, pp. 341–391.
Sanz, J., Chiappe, L., Pérez-Moreno, B., et al., 1996. An early cretaceous bird from Spain and its implications for the evolution of avian flight. Nature 382, 442–445.
Schneider, L., Eggins, S., Maher, W., Vogt, R.C., Krikowa, F., Kinsley, L., Eggins, S.M., da Silveira, R., 2015. An evaluation of the use of reptile dermal scutes as a non-invasive method to monitor mercury concentrations in the environment. Chemosphere 119, 163–169.
Selin, N.E., 2009. Global biogeochemical cycling of mercury: a review. Annu. Rev. Environ. Resour. 34, 43–63.
Shen, J., Feng, Q.L., Algeo, T.J., Liu, J.L., Zhou, C.Y., Wei, W., Liu, J.S., Them, T.R., Gill, B.C., Chen, J.B., 2020. Sedimentary host phases of mercury (Hg) and implications for use of Hg as a volcanic proxy. Earth Planet. Sci. Lett. 543, 116333. https://doi.org/10.1016/j.epsl.2020.116333.
Snyder, R.L., Fiala, J., Bunge, H.J., 2000. Defect and Microstructure Analysis by Diffraction. Oxford University Press, Oxford.
Solé, M., Rödder, D., 2010. Dietary assessments of adult amphibians. In: Amphibian Ecology and Conservation: A Handbook of Techniques, pp. 167–184.
Tcacenco-Manzano, L.M., Fernandes, L.A., 2024. Stratigraphic and cartographic review in the western part of Bauru Basin – Brazil (Upper cretaceous): implications for the depositional model. J. Maps 20. https://doi.org/10.1080/17445647.2024.2308688.
Thibodeau, A.M., Ritterbush, K., Yager, J.A., West, A.J., Ibarra, Y., Bottjer, D.J., Berelson, W.M., Bergquist, B.A., Corsetti, F.A., 2016. Mercury anomalies and the timing of biotic recovery following the end-Triassic mass extinction. Nat. Commun. 7, 11147. https://doi.org/10.1038/ncomms11147.
Thorp, J.L., Van Der Merwe, N.J., 1987. Carbon isotope analysis of fossil bone apatite. S. Afr. J. Sci. 83, 712–715.
US-FDA, F, 2001. Guidance for Industry: Bioanalytical Method Validation. http://www.fda.gov/cder/Guidance/4252fnl.pdf.
Wang, Y., Cerling, T.E., 1994. A model of fossil tooth and bone diagenesis: implications for paleodiet reconstruction from stable isotopes. Palaeogeogr. Palaeoclimatol. Palaeoecol. 107, 281–289.
Weber, M., Weber, K., Winkler, D.E., Tütken, T., 2025. Calcium and strontium isotopes in extant diapsid reptiles reflect dietary tendencies—a reference frame for diet reconstructions in the fossil record. Proc. R. Soc. B Biol. Sci. 292 (2038). https://doi.org/10.1098/rspb.2024.2002, 20242002.
WHO Expert Committee on Specifications for Pharmaceutical Preparations, 1992. Thirty-second report. World Health Organ. Tech. Rep. Ser. 823, 1–134.
Xing, L., Bell, P.R., Persons IV, W.S., Ji, S., Miyashita, T., Burns, M.E., Ji, Q., Currie, P.J., 2012. Abdominal contents from two large early cretaceous compsognathids (Dinosauria: Theropoda) demonstrate feeding on confuciusornithids and dromaeosaurids. PLoS One 7, e44012.
Yap, C.K., Ismail, A., Tan, S.G., Abdul Rabhim, I., 2003. Can the shell of the green-lipped mussel Perna viridis from the west coast of Peninsular Malaysia be a potential biomonitoring material for Cd, Pb, and Zn? Estuar. Coast. Shelf Sci. 57, 623–630.